

Dynamics of Feshbach Molecules in an Ultracold Three-Component Mixture

Alexander Y. Khramov, Anders H. Hansen, Alan O. Jamison, William H. Dowd, and Subhadeep Gupta
Department of Physics, University of Washington, Seattle WA 98195

(Dated: February 21, 2019)

We present investigations of the formation rate and collisional stability of lithium Feshbach molecules in an ultracold three-component mixture composed of two resonantly interacting fermionic ^6Li spin states and bosonic ^{174}Yb . We observe long molecule lifetimes (> 100 ms) even in the presence of a large ytterbium bath and extract reaction rate coefficients of the system. We find good collisional stability of the mixture in the unitary regime, opening new possibilities for studies and probes of strongly interacting quantum gases in contact with a bath species.

Magnetic Feshbach resonances allow precise control of collisional properties, making them a key tool in ultracold atom systems. They have been extensively used to study ultracold molecules, as well as few- and many-body physics [1]. Two-component Fermi gases near a Feshbach resonance provide excellent opportunities to study strongly interacting quantum systems [2]. This is possible due to the remarkable collisional stability of the atom-molecule mixture on the positive scattering length side of the resonance [3, 4], attributed largely to Fermi statistics [5, 6]. Extending the system to three-component mixtures in which only two are resonantly interacting [7] offers the exciting possibility of modifying or probing pairing dynamics by selective control of the third component. A third-component may also be used as a coolant bath for exothermic molecule-formation processes, provided that inelastic processes with the bath are negligible. In the context of many-body physics, a third non-resonant component can be useful as a microscopic probe of superfluid properties [7, 8], as a stable bath for studies of non-equilibrium phenomena [9], or for accurate thermometry of deeply degenerate fermions.

Collisional stability of Feshbach molecules in the absence of Fermi statistics becomes a crucial question for multi-component mixtures [7, 10, 11]. A recent theoretical analysis of such mixtures suggests a possibility for enhanced molecule formation rates with good collisional stability [10]. Enhanced atom loss has been observed near a ^6Li p -wave resonance in the presence of a ^{87}Rb bath [12], while a small sample of the probe species ^{40}K has been found to be stable within a larger strongly interacting ^6Li sample [7].

In this paper we investigate a mixture composed of two resonantly interacting spin states of fermionic ^6Li immersed in a large sample of bosonic ^{174}Yb atoms. While the Li interstate interactions are arbitrarily tunable by means of an s -wave Feshbach resonance at 834 G [13], the interspecies interactions between Li and Yb are constant and small [14]. We present the first observations of formation and evolution of Feshbach molecules in a bath of a second atomic species. In the unitary regime, we observe good collisional stability of the mixture with elastic interactions dominating over inelastic losses. We extract the reaction rate constants from a classical rate equations model of the system.

Our experimental procedure has been described in ear-

lier work [15]. Briefly 3×10^6 atoms of ^{174}Yb in the 1S_0 state and up to 4×10^4 atoms of ^6Li distributed equally between the two $^2S_{1/2}$, $F = \frac{1}{2}$ states (denoted $\text{Li}|1\rangle$, $\text{Li}|2\rangle$), are loaded from magneto-optical traps into a crossed-beam optical dipole trap. We then perform forced evaporative cooling on Yb to the final trap depth $U_{\text{Yb(Li)}} = 15(55) \mu\text{K}$ and mean trap frequency $\bar{\omega}_{\text{Yb(Li)}} = 2\pi \times 0.30(2.4) \text{ kHz}$ [16], during which Li is cooled sympathetically by Yb. Following evaporation, the mixture is held at constant trap depth to allow inter-species thermalization. With a time constant of 1 s the system acquires a common temperature $T_{\text{Yb}} = T_{\text{Li}} = 2 \mu\text{K}$ with atom number $N_{\text{Yb(Li)}} = 2 \times 10^5 (3 \times 10^4)$. This corresponds to $T_{\text{Li}}/T_F \simeq 0.4$, and $T_{\text{Yb}}/T_C \simeq 2.5$, where T_F is the Li Fermi temperature and T_C is the Yb Bose-Einstein condensation temperature [17].

After this initial preparation, we ramp up the magnetic field to a desired value and observe the system after a variable hold time. For fields in the vicinity of the Feshbach resonance, there is a field-dependent number loss

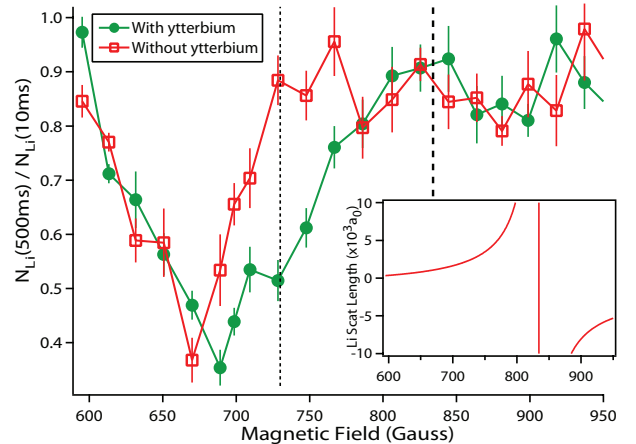
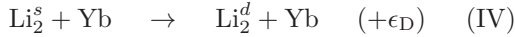
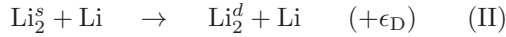


Figure 1: Li atom loss spectroscopy in the presence (filled circles) and absence (open squares) of an Yb bath near the ^6Li 834 G Feshbach resonance (inset). We plot the number of Li atoms after 500 ms of evolution normalized to that at 10 ms. The thick dashed line indicates the resonance center and the thin dashed line indicates the magnetic field at which $\epsilon_B = k_B T_{\text{Li}}$ for the initial conditions.

and heating for the Li cloud during the 20 ms ramp time, resulting in T_{Li} rising to as high as $4.5 \mu\text{K}$. At this point, the average density $\langle n_{\text{Yb(Li)}} \rangle$ is $2.6(0.35) \times 10^{13} \text{ cm}^{-3}$. For interrogation in the absence of the bath, Yb is removed from the trap with a 1 ms light pulse resonant with the $^1S_0 \rightarrow ^1P_1$ transition [18]. Atom number and temperature are monitored using absorption imaging for both species after switching off the magnetic field.

We first present our results on atom loss spectroscopy near the Feshbach resonance (see Fig. 1). The atom-loss maximum obtained in the absence of Yb has been observed previously [13] and can be explained as a result of the formation and subsequent decay of shallow lithium Feshbach dimers [3, 4, 19–21]. In the presence of the Yb bath, the loss feature is shifted and broadened. We interpret the behavior of the mixture in terms of five chemical processes:



Forward process (I) corresponds to a three-body collision event which produces a shallow Feshbach dimer (denoted Li_2^s) accompanied by the release of the dimer binding energy $\epsilon_B = \frac{\hbar^2}{2m_{\text{Li}}a^2}$, where a denotes the $\text{Li}|1\rangle$ - $\text{Li}|2\rangle$ scattering length. Li denotes a ^6Li atom in either of the two spin states. Process (II) corresponds to two-body loss to a deeply bound dimer (denoted Li_2^d) with binding energy ϵ_D . Processes (III) and (IV) are similar to (I) and (II) with the spectator atom being Yb rather than Li. Process (V) corresponds to direct three-body loss to a deeply-bound molecule. Processes (II, IV, V) always result in particle loss from the trap since $\epsilon_D \gg U_{\text{Li}}$. Vibrational relaxation due to collisions between Li_2^s Feshbach molecules may contribute at the lowest fields, but has a negligible rate for the fields at which we perform our analysis [3, 21]. We have experimentally checked that direct three-body loss processes to deeply-bound states involving three Li atoms as well as those involving one Li atom and two Yb atoms are negligible for this work. Three-body losses involving Yb atoms alone have a small effect [22] and are taken into account in our analysis.

In the absence of Yb, only processes (I) and (II) contribute. If we neglect loss process (II), the atom-molecule mixture approaches an equilibrium, characterized by an equality of the forward and reverse rates and an equilibrium molecule fraction $\frac{2N_m}{N_{\text{Li}} + 2N_m} = \left(1 + \frac{e^{-\epsilon_B/k_B T}}{\phi_{\text{Li}}}\right)^{-1}$, where N_m is the molecule number and ϕ_{Li} is the phase space density for each spin component in the ground state of the trap [19–21]. The timescale for achieving equilibrium depends on the three-body rate constant L_3 for process (I), which scales with the scattering length as a^6 , whereas rate constant L_2 for process (II) scales

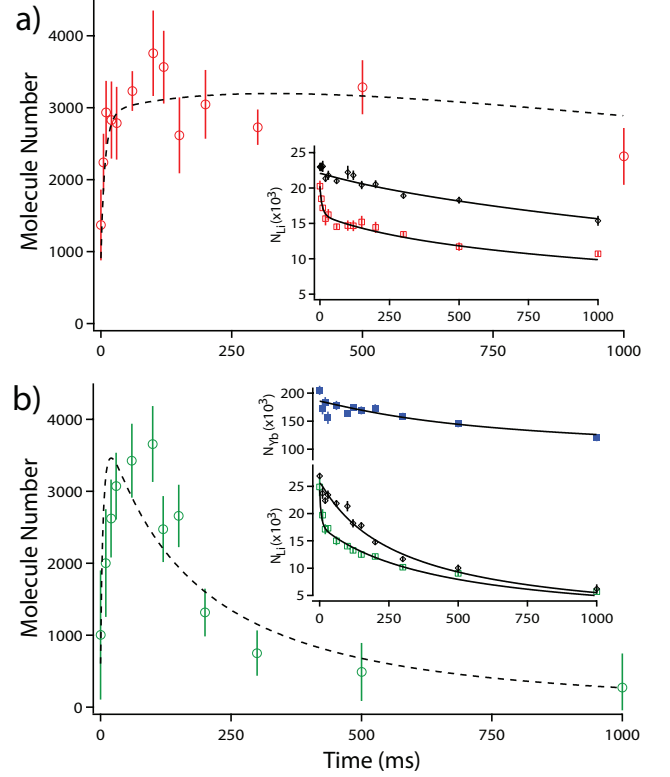


Figure 2: Evolution of Li Feshbach molecule number at 709 G without (a) and with (b) an Yb bath. The numbers are obtained by comparing Li atom numbers (insets) ramped across resonance (diamonds) or not (open squares) as described in the text. Lower inset also shows Yb number (filled squares). The curves are fits with a rate equations-based model.

as $a^{-3.3}$ [23, 24]. The shape of the loss spectrum can thus be qualitatively explained by noting that the dimer formation rate increases with magnetic field while equilibrium dimer fraction and molecule decay rate decrease. The large rate for process (I) at high fields close to resonance ensures equilibrium molecule fraction at all times. Broadly speaking, the rate-limiting step determining the system evolution is the molecule formation rate at low fields and decay rate at high fields. The trap depth also affects the loss spectrum shape, since it determines the magnetic field range over which the formed shallow dimers remain trapped.

In the presence of Yb, the additional dimer formation (III), dimer decay (IV), and 3-body loss (V) processes contribute. The observed loss spectrum is broadened on the higher field side, suggesting that for our parameters, processes (IV) and/or (V) play an important role while process (III) does not. The rate constants L'_3 , L'_2 , and L'_3 , for processes (III), (IV) and (V), have theoretical scalings a^4 , a^{-1} , and a^2 , respectively [10, 23]. Overall, we see two regimes of behavior - a lossy one where molecule formation is energetically favored ($\epsilon_B > k_B T_{\text{Li}}$) and a stable one closer to resonance ($\epsilon_B < k_B T_{\text{Li}}$). The criterion $\epsilon_B = k_B T$ separating these two regimes is equivalent

to $ka = 1$ where $\frac{\hbar^2 k^2}{2m_{\text{Li}}} = k_B T_{\text{Li}}$, i.e., the unitary criterion.

In order to expand upon this qualitative picture, we study the time evolution of the three-component mixture at representative magnetic fields in the above two regimes. We are then able to extract quantitative information for the above processes from a rate-equations model of the system.

Fig. 2 shows the Li atom and molecule number evolution at 709 G ($\epsilon_B = k_B \times 8.3 \mu\text{K}$) where modifications due to the Yb bath are apparent in Fig. 1. The number of Feshbach molecules at a particular field is determined by using a procedure similar to earlier works [3, 4]. After variable evolution time, we ramp the magnetic field with a speed of 40 G/ms either up to 950 G, which dissociates the molecules back into atoms that remain in the trap, or to 506 G, which does not. We then rapidly switch off the magnetic field and image the atomic cloud. The molecule number is obtained from the number difference in the two images (see insets in Fig. 2).

We see that the presence of Yb alters the molecule decay rate while the formation rate is unchanged. The Feshbach molecules appear to coexist for a long time ($> 100\text{ms}$) with the Yb bath, even in the absence of Pauli blocking [10]. We adapt the recent rate-equations analysis of Feshbach losses in a Fermi-Fermi mixture [21] to incorporate a third component, temperature evolution, and trap inhomogeneity. $T_{\text{Li}}/T_F > 0.5$ is satisfied throughout the measurement range, allowing a classical treatment of the Li cloud. We model the density evolutions due to processes (I-V) using:

$$\dot{n}_m = R_m + R'_m - L_2 n_m n_{\text{Li}} - L'_2 n_m n_{\text{Yb}} \quad (1)$$

$$\dot{n}_{\text{Li}} = -2R_m - 2R'_m - L_2 n_m n_{\text{Li}} - 2L'_3 n_{\text{Li}}^2 n_{\text{Yb}} \quad (2)$$

$$\dot{n}_{\text{Yb}} = -L'_2 n_m n_{\text{Yb}} - L'_3 n_{\text{Li}}^2 n_{\text{Yb}}. \quad (3)$$

Here n_m , n_{Li} and n_{Yb} are the densities of shallow dimers Li_2^s , Li atoms and Yb atoms, respectively. $R_m(R'_m) = \frac{3}{4}L_3(L'_3)n_{\text{Li}}^2 n_{\text{Li}}(n_{\text{Yb}}) - qL_3(L'_3)n_m n_{\text{Li}}(n_{\text{Yb}})$ is the net-rate for molecule production via process (I)((III)). We determine q through the constraints on the molecule fraction at equilibrium ($R_m(R'_m) = 0$). We obtain an upper bound for L'_3 by observations at large negative a (described below) which indicates a negligible effect for the data in Fig. 2, allowing us to set $L'_3 = 0$ for the analysis at 709 G.

The time evolution of T_{Li} and T_{Yb} are modeled considering the energy deposition from processes (I) and (III) as well as heating from the density-dependent loss processes (II), (IV) and (V) [25]. In addition, our model also takes into account the effects of evaporative cooling [26], inter-species thermalization [14], one-body losses from background gas collisions, and Yb three-body losses [22, 25]. The Li scattering length at 709 G is $a = 1860 a_0$, ensuring rapid thermalization ($< 1\text{ms}$) in the lithium atom-Feshbach molecule mixture [23]. This allows the assumption of equal temperature T_{Li} to lithium atoms and Feshbach molecules. The heating from molecule-formation at 709 G dominates over inter-species thermalization, maintaining $T_{\text{Li}} \simeq 4.5 \mu\text{K}$ and $T_{\text{Yb}} \simeq 2 \mu\text{K}$, as observed in both experiment and model.

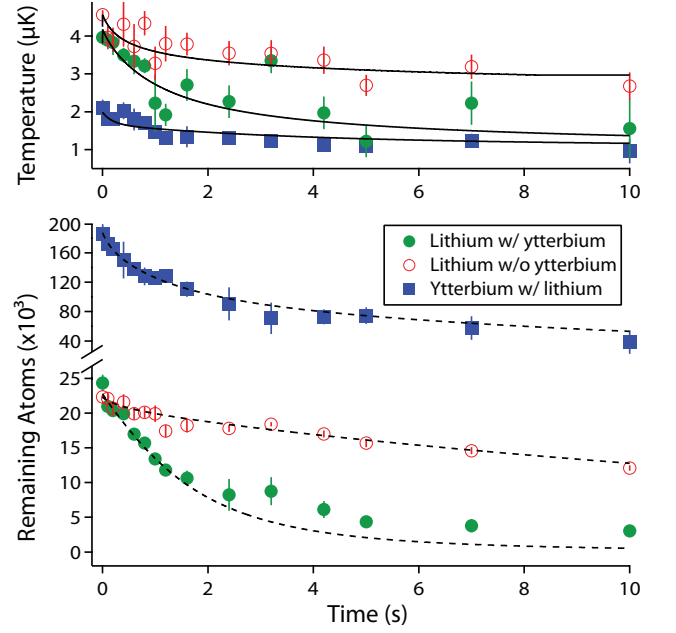


Figure 3: The evolution of temperature and number at 810 G for Li atomic cloud with Yb (filled circles) and without (empty circles) and also for Yb in the presence of Li (filled squares). The curves are fits with a rate equations-based model.

The best-fit rate coefficients extracted from the atom data (shown in the insets) are $L_3 = (1.4 \pm 0.3) \times 10^{-24} \text{ cm}^6/\text{s}$, $L_2 = (1.3 \pm 0.3) \times 10^{-13} \text{ cm}^3/\text{s}$, and $L'_2 = (2.3 \pm 0.2) \times 10^{-13} \text{ cm}^3/\text{s}$. L'_3 is consistent with 0. All reported uncertainties are statistical. The L_3 value is consistent with that obtained in [3], after accounting for the slight differences in experimental parameters. Using $L'_2 \langle n_{\text{Yb}} \rangle$ as a measure of the dimer decay rate, we get 170 ms as the lifetime of a Li Feshbach molecule in the Yb bath.

We now turn to the unitary regime, where we choose 810 G ($ka = +6$, $\epsilon_B = k_B \times 0.11 \mu\text{K}$) as our representative field to study the mixture properties. It is difficult to reliably observe the molecule number using our earlier method in this regime, so we only monitor the atoms (see Fig. 3). Starting with an inter-species temperature differential as before, we observe a fast drop in T_{Li} in the presence of Yb and clear evidence of inter-species thermalization. The Li number in the three-component mixture exhibits a long $1/e$ lifetime of 2 s, far larger than at 709 G. However this is still an order of magnitude shorter than that obtained in the absence of Yb. The interpretation of the decay is not straightforward as both two-body (process (IV)) and three-body (process (V)) inelastic loss can contribute [7, 27]. The large rate for process (I) in this regime ensures equilibrium molecule fraction at all times. By fitting to data taken at 935 G where $ka = -2$ and process (V) is expected to dominate inelastic loss, we obtain $L'_3 = (4.3 \pm 0.3) \times 10^{-28} \text{ cm}^6/\text{s}$. This sets a lower bound for L'_3 at 810 G. We fit the first 2.5 s of data

in Fig. 3 after fixing L_2' to its value scaled from 709 G and find $L_3^d = (9.5 \pm 0.5) \times 10^{-28} \text{ cm}^6/\text{s}$ at 810 G. The slight disagreement in Li atom number at long times may be due to a small ($< 10\%$) inequality in our spin mixture composition, which the model does not take into account.

The qualitative features of both spectra in Fig. 1 can be theoretically reproduced by using field-dependent reaction coefficients scaled from our measured values at 709 and 810 G. However, a full quantitative comparison will need to take into account the theoretical deviations from scaling behavior in the unitary regime as well as experimental variations in the initial temperature, and is open to future investigation.

By extending the forced evaporative cooling step, lower temperature mixtures can be produced where bosonic ^{174}Yb shrinks to a size smaller than the Fermi diameter of the ^6Li cloud. Such experiments at 834 G yield $T_{\text{Li}}/T_F \simeq 0.25$ with $N_{\text{Yb}} = N_{\text{Li}} = 2.5 \times 10^4$. Here, the estimated volume of the Yb sample is $\simeq 0.3$ of the Li sample volume, compared to 3.3 in the classical regime. The mixture is thus also capable of achieving the opposite regime of a second species being immersed inside a strongly interacting quantum degenerate Fermi gas, similar to earlier studies in the K-Li mixture [7].

Our experiments with the Yb-Li mixture near a Fesh-

bach resonance demonstrate effects of an additional species on chemical reaction rates in the microKelvin regime. We observe a long lifetime for Feshbach molecules, even in the absence of Pauli blocking. Our demonstrated stability of the mixture near the unitary regime of the resonance opens various possibilities of studying strongly interacting fermions immersed in a bath species or being interrogated by a small probe species. Future experimental opportunities include realizations of non-equilibrium states, and studies of superfluid properties, for instance by controlled relative motion between the two species. Finally, our results constitute an advance in the manipulation of ultracold mixtures of alkali and alkaline-earth-like atoms [15, 28]. These mixtures may be used to produce quantum gases of paramagnetic polar molecules which are promising for diverse applications such as quantum simulation of lattice spin models [29], tests of fundamental symmetries [30], and probes of time variations in fundamental constants [31].

We thank Ben Plotkin-Swing for experimental assistance, and J.P. D’Incao, T.-L. Ho and M.W. Zwierlein for helpful discussions. We gratefully acknowledge support from the National Science Foundation and the Air Force Office of Scientific Research. A.K. thanks the NSERC.

-
- [1] C. Chin, R. Grimm, P. S. Julienne, and E. Tiesinga, *Rev. Mod. Phys.* **82**, 1225 (2010).
 - [2] S. Giorgini, L. P. Pitaevskii, and S. Stringari, *Rev. Mod. Phys.* **80**, 1215 (2008).
 - [3] S. Jochim, M. Barternstein, A. Altmeyer, G. Hendl, C. Chin, J. Hecker Deschlag, and R. Grimm, *Phys. Rev. Lett.* **91**, 240402 (2003).
 - [4] J. Cubizolles, T. Bourdel, S. J. J. M. F. Kokkelmans, and C. Salomon, *Phys. Rev. Lett.* **108**, 043201 (2012).
 - [5] B. D. Esry, C. H. Greene, and H. Suno, *Phys. Rev. A* **65**, 010705(R) (2001).
 - [6] D. S. Petrov, C. Salomon, and G. V. Shlyapnikov, *Phys. Rev. Lett.* **93**, 090404 (2004).
 - [7] F. Spiegelhalder, A. Trenkwalder, D. Naik, G. Hendl, F. Schreck, and R. Grimm, *Phys. Rev. Lett.* **103**, 223203 (2009).
 - [8] K. Targonska and K. Sacha, *Phys. Rev. A* **82**, 033601 (2010).
 - [9] A. Robertson and V. M. Galitski, *Phys. Rev. A* **80**, 063609 (2009).
 - [10] J. P. D’Incao and B. D. Esry, *Phys. Rev. Lett.* **100**, 163201 (2008).
 - [11] J. J. Zirbel, K.-K. Ni, S. Ospelkaus, J. P. D’Incao, C. E. Wieman, J. Ye, and D. S. Jin, *Phys. Rev. Lett.* **100**, 143201 (2008).
 - [12] B. Deh, C. Marzok, C. Zimmermann, and P. W. Courteille, *Phys. Rev. A* **77**, 010701(R) (2008).
 - [13] K. Dieckmann, C. A. Stan, S. Gupta, Z. Hadzibabic, C. H. Schunck, and W. Ketterle, *Phys. Rev. Lett.* **89**, 203201 (2002).
 - [14] V. V. Ivanov, A. Khramov, A. H. Hansen, W. H. Dowd, F. Münchow, A. O. Jamison, and S. Gupta, *Phys. Rev. Lett.* **106**, 153201 (2011).
 - [15] A. H. Hansen, A. Khramov, W. H. Dowd, A. O. Jamison, V. V. Ivanov, and S. Gupta, *Phys. Rev. A* **84**, 011606(R) (2011).
 - [16] The optical trap wavelength = 1064 nm, initial power = 10 W per beam, waist = $26 \mu\text{m}$, crossing angle = 20° . During the evaporative cooling step, the power is reduced by a factor of 16 over 3 s. At the highest optical trap powers, $\bar{\omega}_{\text{Yb}}/\bar{\omega}_{\text{Li}} = 0.12$ and $U_{\text{Yb}}/U_{\text{Li}} = 0.45$. At the lower final power, gravity reduces the effective trap depth of the heavier component more, but has negligible effect on the frequency ratio.
 - [17] By continuing the forced evaporation to lower trap depths, our apparatus can produce pure Yb BECs with $> 2 \times 10^5$ atoms in single-species experiments and deeply Fermi degenerate gases $T_{\text{Li}}/T_F \simeq 0.1$ in two-species experiments.
 - [18] This step is carried out either immediately before or after the field ramp, with no discernible difference in lithium number or temperature between the two.
 - [19] C. Chin and R. Grimm, *Phys. Rev. A* **69**, 033612 (2004).
 - [20] S. J. J. M. F. Kokkelmans, G. V. Shlyapnikov, and C. Salomon, *Phys. Rev. A* **69**, 031602(R) (2004).
 - [21] S. Zhang and T.-L. Ho, *New J. Phys.* **13**, 055003 (2011).
 - [22] Y. Takasu, K. Maki, K. Komori, T. Takano, K. Honda, M. Kumakura, T. Yabuzaki, and Y. Takahashi, *Phys. Rev. Lett.* **91**, 040404 (2003).
 - [23] D. S. Petrov, *Phys. Rev. A* **67**, 010703(R) (2003).
 - [24] J. P. D’Incao and B. D. Esry, *Phys. Rev. Lett.* **94**, 213201 (2005).
 - [25] T. Weber, J. Herbig, M. Mark, H.-C. Naegerl, and R. Grimm, *Phys. Rev. Lett.* **91**, 123201 (2003).

- [26] K. M. O'Hara and J. E. Thomas, Phys. Rev. A. **64**, 051403(R) (2001).
- [27] X. Du, Y. Zhang, and J. E. Thomas, Phys. Rev. Lett. **102**, 250402 (2009).
- [28] H. Hara, Y. Takasu, Y. Yamaoka, J. M. Doyle, and Y. Takahashi, Phys. Rev. Lett. **106**, 205304 (2011).
- [29] A. Micheli, G. K. Brennen, and P. Zoller, Nature Physics **2**, 341 (2006).
- [30] J. J. Hudson, D. M. Kara, I. J. Smallman, B. E. Sauer, M. R. Tarbutt, and E. A. Hinds, Nature **473**, 493 (2011).
- [31] M. Kajita, G. Gopakumar, M. Abe, and M. Hada, Phys. Rev. A **84**, 022507 (2011).